Orientational exchange approach to fluorescence anisotropy decay

David W. Piston and Enrico Gratton
Department of Physics, Laboratory for Fluorescence Dynamics, University of Illinois at Urbana-Champaign, Urbana, Illinois 61801

ABSTRACT Fluorescence depolarization is a powerful technique in resolving dynamics of molecular systems. Data obtained in fluorescence depolarization experiments are highly complex. Mathematical models for analyzing data from depolarization due to rotational motion have been largely based on the rotational diffusion equation. These results have been verified by Monte Carlo simulations. It has been implicitly stated that a 90° jump model between predefined orientations such as presented by G. Weber (1971. *J. Chem. Phys.* 55:2399–2411) should, for the specific case of fluorescence depolarization, give the same answer as the diffusion equation. Since the highly symmetric cases considered by G. Weber gave the same result as the diffusion equation, it has been desirable to use this method in cases where depolarization arises from both discrete processes and rotational diffusion. We have derived, in a compartmental formalism, the general result for excitation and emission dipoles not necessarily coincident with any of the principal rotational axes of the fluorophore from this exchange model, and have found it to be different from that of the diffusion equation approach. We have also verified this difference with a Monte Carlo simulation of our exchange model. This derivation allows us to define the limits of validity of the 90° exchanges to model rotational diffusion. Also, for systems where movements may be jumps between a few preferred orientations, the actual physical mechanism of depolarization may not be accurately represented by continuous diffusion. The compartmental formalism developed here can be used to easily combine rotational motions with discrete position jumps or other level kinetics. While the difference between the diffusion equation and random walk of finite step size derivations has been presented for observations of different order properties for the compartmental formalism, we discuss the possibility of finding this difference by using the ratio of relaxation rates from a single experiment. Also, the temperature dependence of the exchange rates is calculated in relation to the Kramer's theory.

INTRODUCTION

The study of fluorescence depolarization is a very powerful technique in resolving dynamics of molecular systems. Information about the size and shape of a molecule, as well as its interaction with the surrounding solvent and with other molecules, can be obtained. Techniques to measure these effects have been used in both the time and frequency domains to study a wide range of systems from proteins (1–3) to liquid crystals and lipid bilayers (4, 5). The data obtained in fluorescence depolarization experiments is highly complex, and may be further complicated by a variety of factors such as multiple fluorescence lifetimes, excited-state reactions, energy transfer, and solvent interactions. In this paper we will consider only fluorescence depolarization caused by rotational motions of the emitting molecule. For nonspherical molecules, the anisotropy decay will be multiexponential or nonexponential. Due to this complexity, researchers are interested in models that predict the polarization anisotropy decay for nonisotropic rotations. Here we are interested in the limits of validity of two separate theoretical derivations of fluorescence depolarization decay due to anisotropic rotations, that is, rotations of nonsymmetric molecules. For this purpose, we are limiting ourselves to derivation for unrestricted rotations where the shape of the molecule is the only factor that contributes to the depolarization. We will consider first the mathematical forms of the depolarization given by the two methods, and then we will examine the differences and similarities between them with particular emphasis on the different physical assumptions of the two approaches.

Mathematical models used to describe fluorescence anisotropy decay were based on either the diffusion

Dr. Piston's present address is School of Applied and Engineering Physics, Cornell University, Clark Hall, Ithaca, NY 14853.
Address correspondence to Dr. Gratton.

0006-3495/89/12/1083/09 $2.00

equation (6) or discontinuous "jumps" between orientations, as used by G. Weber (7). Models using the diffusion equation are based on the original derivation of rotational diffusion by Favro (8). For cases where the absorption and emission dipoles are colinear and aligned with one of the principal axes of the molecule (called the "aligned case"), these two derivations give the same result regardless of the shape of the molecule. The mathematical form given by both models in the aligned case is the sum of two exponential terms, with each method yielding the same preexponential factors and rotational correlation rates. In the aligned case, the preexponentials are independent of the diffusion constants and geometrical factors, and the rotational correlation rates are $6D \pm 2\Delta$ where

$$D = \tfrac{1}{3}(D_x + D_y + D_z)$$

$$\Delta = (D_x^2 + D_y^2 + D_z^2 - D_xD_y - D_yD_z - D_zD_x)^{1/2}.$$

Here, D_i is the rotational diffusion constant or rotational rate about the ith axis, D is their average, and Δ is related to the anisotropy of the rotations. Each of these two rotational correlation times are symmetric with respect to the three principal axes of the molecule. From the diffusion equation derivation, the anisotropy decay in the general nonaligned case is known to be a sum of five exponential terms. The three extra correlation times found in this case are not symmetric in the diffusion rates, and we call them the "cross-terms." The cross-terms do not appear in the aligned case because their preexponentials are zero under these conditions. The full expressions for the anisotropy decay from both derivations are given in Theory. The discontinuous jump model between orientations was never generalized to the nonaligned case (neither absorption nor emission dipoles aligned with one of the principal axes) and therefore no solution is available that provides the five exponential terms found using the diffusion equation approach. Perhaps because of the lack of a general solution for anisotropic rotations from the discontinuous model, the diffusion equation has been used as the only mathematical model of rotational motion (9). The results of the diffusion equation derivations were quickly verified by many researchers (10, 11) and have since been verified by Monte Carlo simulations (12). In addition, it has been implicitly stated in some of these papers that if the nonalignment of dipoles and prinicipal diffusion axes were taken into account, Weber's method should give the same five exponential answer as the diffusion equation (10), and the question has been raised as to the limits of validity of the discontinuous approach (13, 14). The equivalence of jump and diffusion models has also been assumed to be true in the field of dipolar relaxation as long as detailed balance is upheld (15, 16). Since unrestricted rotations should not be affected by electronic transitions, they will always meet this criterion and we therefore would expect both methods to give the same result. Since the pioneering work of Weber using a jump model, it has been desirable to use his unique approach to analyze systems where depolarization results from a combination of rotations and processes that are compartmental by nature, such as some cases of dipolar relaxation, energy transfer, or reorientation induced by the change in dipole moment. Great effort has been expended to combine rotational motion with level kinetics using the diffusion equation, but the expressions obtained are complicated and difficult to apply to an experimental situation (17, 18). The purpose of this paper is to examine the applicability and limitations of a compartmental formalism to describe rotations that may be diffusive. We do not believe that the actual physical process of rotations is ever only 90° jumps, but we do wish to take advantage of the mathematical coincidence between the compartmental and diffusion equation approaches when it occurs. The compartmental approach will allow us to easily add processes that contribute to the anisotropy decay in a naturally compartmental way. This approach has previously been used to fit frequency domain anisotropy decay data directly to a physical model (13).

We have expanded Weber's approach to the general nonaligned case and derived the general result of the 90° jump model. We find the result to be different from that of the diffusion equation approach. While both models give five exponential terms for the nonaligned case, the rotational correlation times of the cross terms derived in the discontinuous model are not equivalent to those found with the diffusion equation approach. Instead, the preexponentials are each the same for both models, since for the three cross terms they arise from only geometrical factors and initial conditions. We have also verified our compartmental model result with a Monte Carlo simulation of 90° jumps between orientations. Our results demonstrate that the original agreement between the two methods in the aligned case was only a coincidence arising from the fact that the preexponential factors of the three cross terms are zero in both solutions for this case.

This difference is significant for two main reasons. First, for systems where the fluorophore is small and may not be very much larger than the solvent molecules, the actual physical mechanism of rotation may be large jumps instead of continuous diffusion. In this case, the jumps should be treated in a random walk formalism of finite step size. The differences between this random walk approach and continuous diffusion have been discussed in the literature (19). Second, in systems where a small number of specific orientations may be preferred due to environmental constraints on the fluorophore, a major driving force of depolarization may be jumps between

these preferred states. In both of these cases, the solution and physical implications given by a diffusion equation approach may be incorrect.

In this paper, we outline the assumptions and show the results of both methods, as well as detail the formalism used to calculate fluorescence depolarization with a compartmental model and show the specific mathematics used in the jump model derivation for a general geometry. We also describe the procedure and results for the Monte Carlo simulation of the 90° jump model, and discuss the significance of the differences and similarities between the two models, as well as the assumptions about the physical mechanism of rotation that is used in each model. We will also pay particular attention to the case of restricted motions and to the temperature dependence of the rotational rates in each of the two approaches.

THEORY

We first briefly describe the results for rotational motion that are derived using the diffusion equation. For this, we will follow the assumptions and notation of Chaung and Eisenthal (10). Their derivation begins with the rotational diffusion equation as given by Favro (8):

$$\partial f(\Omega, t)/\partial t = -Hf(\Omega, t), \tag{1}$$

with the Hamiltonian given by:

$$H = \sum_i D_i L_i^2, \tag{2}$$

where D_i is the ith component of the diagonalized diffusion tensor, and L is the quantum mechanical angular momentum operator. The function, f, in Eq. 1 may be solved by the Green's function method. This function multiplied by the probability of absorption is then integrated over the sphere of possible dipole directions for each of the parallel and perpendicular intensities; in the case of a macroscopically nonaligned sample, the original dipole distribution is uniform. The geometry of the system is defined by the projection of the unit vector of the absorption dipole along the molecular axes to be γ_x, γ_y, γ_z. The corresponding components of the emission dipole are denoted as q_x, q_y, q_z. The result for the time-resolved anisotropy, $r(t)$, is then given by:

$$\begin{aligned} r(t) = {}& {}^3/_{10}[4\, q_x q_y \gamma_x \gamma_y e^{-3(D_z+D)t} \\ & + 4\, q_y q_z \gamma_y \gamma_z e^{-3(D_x+D)t} \\ & + 4\, q_z q_x \gamma_z \gamma_x e^{-3(D_y+D)t} \\ & + (\beta + \alpha) e^{-(6D+2\Delta)t} \\ & + (\beta - \alpha) e^{-(6D-2\Delta)t}], \end{aligned} \tag{3}$$

where

$$\begin{aligned} \beta = {}& q_x^2\gamma_x^2 + q_y^2\gamma_y^2 + q_z^2\gamma_z^2 - {}^1/_3 \\ \alpha = {}& \left(\frac{D_x}{\Delta}\right)(q_y^2\gamma_y^2 + q_z^2\gamma_z^2 - 2\,q_x^2\gamma_x^2 + \gamma_x^2 + q_x^2) \\ & + \left(\frac{D_y}{\Delta}\right)(q_z^2\gamma_z^2 + q_x^2\gamma_x^2 - 2\,q_y^2\gamma_y^2 + \gamma_y^2 + q_y^2) \\ & + \left(\frac{D_z}{\Delta}\right)(q_x^2\gamma_x^2 + q_y^2\gamma_y^2 - 2\,q_z^2\gamma_z^2 + \gamma_z^2 + q_z^2) \\ & - \left(\frac{2\,D}{\Delta}\right) \end{aligned}$$

and with D and Δ as defined in the Introduction. This is valid only in the case $\Delta \neq 0$; for $\Delta = 0$ one must simplify the expression before solving the diffusion equation, and the α term disappears.

We will now describe our implementation of a compartmental jump model. First, we will outline the formalism used to calculate fluorescence anisotropy using this model, and then describe the assumptions and specific equations used in the general case of an anisotropic ellipsoid with neither absorption nor emission necessarily aligned with a principal axis of the molecule. We will use the same notation described above.

The formalism for using a compartmental model to calculate fluorescence depolarization has been previously outlined (13) and is presented here as a convenience to the reader. In general, to implement the compartmental model for n compartments, we use the following procedure. First we must define a state vector, **S**, which contains n entries, one for each compartment. A compartment is simply one state of the basis set of distinguishable polarizations. These compartments can represent different spatial orientations of the system, or possible excited-state products. Next, we define a matrix of population and depopulation rates for each compartment:

$$\mathbf{A} = \begin{pmatrix} -k_1 - \Sigma\, k_{i1} & k_{12} & \cdots & k_{1n} \\ k_{21} & -k_2 - \Sigma\, k_{i2} & \cdots & k_{2n} \\ \vdots & \vdots & \ddots & \vdots \\ k_{n1} & k_{n2} & \cdots & -k_n - \Sigma\, k_{in} \end{pmatrix}, \tag{4}$$

where k_i is the decay rate of the ith compartment and k_{ij} is the rate of interconversion from the jth to the ith compartment. This matrix contains only constant rates, which can be interconversion rates or decay rates. An initial condition vector, **B**, which contains the initial excited population of each compartment, must be determined. For fluorescence depolarization experiments the initial populations are given by the dipole selection law

under excitation by polarized light. The application of this photoselection in the general case will be described later. Once we have defined these quantities, we can solve the eigenvalue problem $\mathbf{AS} = \lambda\mathbf{S}$ with boundary conditions, **B**. This type of matrix always gives real and positive eigenvalues (20). In the case of larger matrices, we can easily solve the eigenvalue problems numerically on a computer. The resulting λ_i's give the decay associated rates, and the eigenvectors, E_i, will lead to the preexponentials as shown below. The E_i's each have j components, E_{ij}. Since we would like to use this method to calculate anisotropy decay, we must introduce our experimental geometries to the model. We define two polarization vectors, $P_\perp$ and $P_\parallel$, such that the j_{th} component of $P_\perp$ is the relative perpendicular contribution to the fluorescence intensity of the jth compartment and the same for $P_\parallel$. These vectors are defined by the experimental geometry of the observation of the emission dipole, and are multiplied by the E_i's to obtain the preexponential factors. We can then use the results of our eigenvalue problem, along with the P vectors, to calculate $I_\parallel(t)$, $I_\perp(t)$ and the total intensity, $I(t)$, with the following formulae:

$$I_\parallel(t) = \sum_{i=1}^{n} e^{-\lambda_i t} \sum_{j=1}^{n} P_{\parallel j} E_{ij} \tag{5}$$

$$I_\perp(t) = \sum_{i=1}^{n} e^{-\lambda_i t} \sum_{j=1}^{n} P_{\perp j} E_{ij} \tag{6}$$

$$I(t) = I_\parallel(t) + 2I_\perp(t) \tag{7}$$

and of course the time-resolved anisotropy,

$$r(t) = \frac{I_\parallel(t) - I_\perp(t)}{I_\parallel(t) + 2I_\perp(t)}. \tag{8}$$

As mentioned above, the initial conditions for the fluorescence intensity come from the dipole absorption law, which goes as the average of $\cos^2$ of the angle between the absorption dipole and the direction of polarization over the initial distribution of dipoles. To calculate the initial intensity, we must also include the projections of the dipole emission in both the parallel and perpendicular directions. However, because we would like to fit data with this method, we derive the boundary conditions for both colinear absorption and emission dipoles, and then include any difference between them in the P vectors. This is done because the gradient of variables contained in the boundary conditions of an eigenvalue problem are irregular, making a least-squares minimization difficult. To derive the initial conditions, we use the spherical coordinates θ for the angle between the vector and the z-axis, and ϕ for the angle from the vector's projection on the x-y plane to the x-axis. Our experimental condition is for light arriving from the positive x-direction polarized along z. In this paper we are considering only isotropic (nonaligned) samples, so we must integrate the $\cos^2\theta$ absorption over all dipole orientations with a uniform distribution of dipoles, as was done in the diffusion equation approach. For the initial intensity of the basis compartment with dipole along the z-axis this integral is,

$$B_z = \int_0^{2\pi} d\phi \int_0^{\pi} \sin\theta\, d\theta \cos^2\theta (\hat{r} \cdot \hat{z})^2, \tag{9}$$

where the first term, $\cos^2\theta$, is the probability of exciting a dipole with angle θ from the excitation polarization (in our geometry this is the z-axis), and the second term, $(\hat{r} \cdot \hat{z})^2$, gives the intensity projection of the dipole on the z-axis. For B_z we use the identity $\hat{r}_z = \cos\theta\hat{z}$, and this integral reduces to,

$$B_z = 2\pi \int_0^{\pi} \sin\theta\, d\theta \cos^4\theta = \frac{4\pi}{5}. \tag{10}$$

This calculation is the same for the initial populations along the x- and y-axes by noting the two identities $\hat{r}_y = \sin\theta \sin\phi\hat{y}$ and $\hat{r}_x = \sin\theta \cos\phi\hat{x}$. The values are equal and are both $4\pi/15$. Because only the relative populations of each compartment are important to the anisotropy calculation, we normalize the initial conditions so the sum of the initial intensities is equal to one. In the laboratory frame, there are two distinguishable compartments along each axis, one for each absorption and emission dipole plane (7). Since we assume a uniform initial distribution of dipoles, the initial intensities are not dependent on the shape of the molecule or location of the dipole in the molecular frame. We can thus define the initial values by these six distinguishable states. The normalized initial values we use are 0.3 for the two states with absorption dipoles along the laboratory z-axis and 0.1 for each of the four states with absorption dipoles along the x- and y-axes. However, the rotations are about the principal axes in the molecular frame, so each initial population must be rotated in the molecular frame separately and then transformed back into the lab frame to calculate the observed fluorescence anisotropy. Once we have calculated the time-resolved anisotropy, we can then integrate over all time to obtain the steady-state values.

To calculate the fluorescence depolarization for the general molecular case (where the absorption and emission dipoles and the principal axes of rotation may all be nonaligned) with a compartmental analysis approach we use a state vector of 24 components as the basis set of rotations in the molecular frame. These 24 states represent all of the possible orientations of a general dipole that are reachable by a series of 90° rotations along the principal axes in the molecular frame. The 24 comes from the three possible alignments of a vector in each of the

TABLE 1 Rotation matrix, A, and state vector, S, for the 24 × 24 case, with $Q = k_f + 2D_x + 2D_y + 2D_z$

$-Q$	0	0	0	0	0	0	0	0	0	0	0	D_x	D_x	0	0	0	D_z	D_z	0	D_y	0	D_y	0	1	2	3
0	$-Q$	0	0	0	0	0	0	0	0	0	0	D_x	D_x	0	0	D_z	0	0	D_z	0	D_y	0	D_y	1	−2	−3
0	0	$-Q$	0	0	0	0	0	0	0	0	0	0	0	D_x	D_x	D_z	0	0	D_z	D_y	0	D_y	0	−1	2	−3
0	0	0	$-Q$	0	0	0	0	0	0	0	0	0	0	D_x	D_x	0	D_z	D_z	0	0	D_y	0	D_y	−1	−2	3
0	0	0	0	$-Q$	0	0	0	0	0	0	0	D_y	D_y	0	D_x	0	D_x	0	D_z	D_z	0	0	3	1	2
0	0	0	0	0	$-Q$	0	0	0	0	0	0	D_y	0	0	D_y	0	D_x	0	D_x	D_z	D_z	0	0	3	−1	−2
0	0	0	0	0	0	$-Q$	0	0	0	0	0	D_y	0	0	D_y	D_x	0	D_x	0	0	0	D_z	D_z	−3	1	−2
0	0	0	0	0	0	0	$-Q$	0	0	0	0	D_y	D_y	0	0	D_x	0	D_x	0	0	D_z	D_z	−3	−1	2
0	0	0	0	0	0	0	0	$-Q$	0	0	0	D_z	0	D_z	0	D_y	D_y	0	0	0	D_x	D_x	0	2	3	1
0	0	0	0	0	0	0	0	0	$-Q$	0	0	D_z	0	D_z	D_y	D_y	0	0	D_x	0	0	D_x	2	−3	−1
0	0	0	0	0	0	0	0	0	0	$-Q$	0	D_z	0	D_z	0	0	0	D_y	D_y	D_x	0	0	D_x	−2	3	−1
0	0	0	0	0	0	0	0	0	0	0	$-Q$	0	D_z	0	D_z	0	0	D_y	D_y	0	D_x	D_x	0	−2	−3	1
D_x	D_x	0	0	0	D_y	D_y	0	D_z	0	D_z	0	$-Q$	0	0	0	0	0	0	0	0	0	0	0	1	3	−2
D_x	D_x	0	0	D_y	0	0	D_y	0	D_z	0	D_z	0	$-Q$	0	0	0	0	0	0	0	0	0	0	1	−3	2
0	0	D_x	D_x	D_y	0	0	D_y	D_z	0	D_z	0	0	0	$-Q$	0	0	0	0	0	0	0	0	0	−1	3	2
0	0	D_x	D_x	0	D_y	D_y	0	0	D_z	0	D_z	0	0	0	$-Q$	0	0	0	0	0	0	0	0	−1	−3	−2
0	D_z	D_z	0	D_x	0	D_x	0	D_y	D_y	0	0	0	0	0	0	$-Q$	0	0	0	0	0	0	0	2	1	−3
D_z	0	0	D_z	0	D_x	0	D_x	D_y	D_y	0	0	0	0	0	0	0	$-Q$	0	0	0	0	0	0	2	−1	3
D_z	0	0	D_z	D_x	0	D_x	0	0	0	D_y	D_y	0	0	0	0	0	0	$-Q$	0	0	0	0	0	−2	1	3
0	D_z	D_z	0	0	D_x	0	D_x	0	0	D_y	D_y	0	0	0	0	0	0	0	$-Q$	0	0	0	0	−2	−1	−3
D_y	0	D_y	0	D_z	D_z	0	0	0	D_x	D_x	0	0	0	0	0	0	0	0	0	$-Q$	0	0	0	3	2	−1
0	D_y	0	D_y	D_z	D_z	0	0	D_x	0	0	D_x	0	0	0	0	0	0	0	0	0	$-Q$	0	0	3	−2	1
D_y	0	D_y	0	0	0	D_z	D_z	D_x	0	0	D_x	0	0	0	0	0	0	0	0	0	0	$-Q$	0	−3	2	1
0	D_y	0	D_y	0	0	D_z	D_z	0	D_x	D_x	0	0	0	0	0	0	0	0	0	0	0	0	$-Q$	−3	−2	−1

eight octants of three dimensional space. This rate matrix of interconversions and state vector is shown in Table 1. The rotational matrix is the compilation of all the 90° rotations about each principal axis of the molecule. The 24 states are denoted by the position of the principal molecular axes with respect to the initial orientation of the molecule. Since we consider only 90° jumps, the molecular frame remains the same except for exchanges of axes. For example, if the beginning state of (1, 2, 3) is rotated about the molecular x-axis in the right-hand (+) direction, the final state is (1, 3, −2). This is shown in Fig. 1. Note that we use the "right-hand rule" to denote the positive direction about an axis. In previous 90° jump model calculations only six compartments have been used

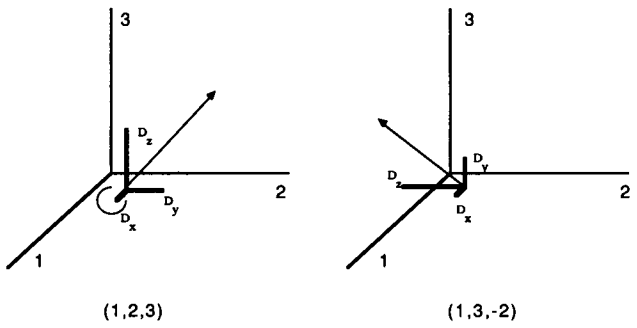

FIGURE 1 Rotation about the x-axis of a molecule with principal rotation rates D_x, D_y, D_z, from state (1, 2, 3) to state (1, 3, −2). Also shown is the resulting movement of a dipole, μ.

(7). The use of the six states is indeed justified by the amount of molecular symmetry assumed in those derivations. However, in the case where the rotational axes are not necessarily aligned with the dipole, there are 24 distinguishable rotational states instead of only six. Due to the initial intensity considerations mentioned above, we break the problem into six parts, each using the same 24 × 24 matrix to evolve the initial vector in time. There are six distinguishable initial basis states of a uniform distribution of absorption–emission dipole pairs. Since with anisotropic rotations a dipole initially aligned with the laboratory z-axis will not necessarily ever align with the x-axis via a series of 90° rotations, it may happen that there is no mixing of the initial states, so we must therefore consider each of these six initial states separately. The rotational motions, as opposed to the initial conditions, are independent of the laboratory frame, and depending on the shape of the molecule and the location of the dipoles, may have up to 24 distinguishable basis states. Since the initial distribution of dipoles is defined by the laboratory frame, we can determine the transformation matrices between each of the six initial ensembles and the laboratory axes. The **P** vectors are then determined by using these transformations to rotate the 24 states of molecular frame rotation into the laboratory frame separately for each of the six initial ensembles. The components of the **P** vectors are the square of the projections of these rotated vectors in each of the parallel and perpendicular directions. After defining our compartmental matrix, initial conditions, and the **P** vectors, we

can run the eigenvalue–eigenvector solver once and multiply each eigenvector by its initial factors. These initial factors are either 0.3 or 0.1. The $I_{\parallel}(t)$ and $I_{\perp}(t)$ values are now calculated in the same manner as shown above, but now there are six separate sets of eigenvectors and P vectors that must be added.

Shown here are the results from our eigenvalue–eigenvector problem (Table 2). The values for the eigenvalues were determined analytically using Mathematica (Wolfram Research, Champaign, IL) on an AT&T UNIX PC. The values listed in this table under $\parallel$ and $\perp$ correspond to the second summations (over j) of Eqs. 5 and 6. These parameters are combinations of several eigenvector, **P** vector products and have been determined somewhat empirically. The results from the diffusion equation are given in Eq. 3. For the compartmental case, after applying the initial conditions, we get five nonzero, preexponential terms, plus the total intensity decay term which cancels out in the anisotropy calculation. Although the 144 terms prohibit us from obtaining a true analytical solution for the eigenvectors, we can graph the preexponential terms versus each γ_x, γ_y, γ_z, q_x, q_y, q_z. From these graphs (not shown), we see that regardless of the γ and q values, all of the five preexponentials agree between the two models. Since the preexponentials of the cross terms come only from geometrical factors and do not contain diffusional constants, this indicates that we have the geometry of the system correct. As stated above, we observe that two of the rates, $(6\,D \pm 2\,\Delta)$, are the same in each of the two independent derivations. It is these two rates which remain observable regardless of the alignment of the absorption and emission dipoles. The only difference between the two solutions is in the exponential part of the cross-terms (the first three exponential terms of Eq. 3). The diffusion equation yields rotational correlation rates of $4\,D_i + D_j + D_k$, where i, j, k are the three cyclic permutations of x, y, z. Our solution, using the compartmental approach, gives rates of $4\,D_i + 2\,D_j + 2\,D_k$. This extra factor of two causes the jump model to show faster depolarization than the diffusion model.

TABLE 2. Eigenvalues and their degeneracy for the general jump model matrix

Rate	Degeneracy	Parallel	Perpendicular
k_f	1	1/9	1/9
$6D + 2\Delta$	2	$(1/15)(\beta + \alpha)$	$-(1/30)(\beta + \alpha)$
$6D - 2\Delta$	2	$(1/15)(\beta - \alpha)$	$-(1/30))\beta - \alpha)$
$4D_x + 2D_y + 2D_z$	3	$(4/15)q_yq_z\gamma_y\gamma_z$	$-(2/15)q_yq_z\gamma_y\gamma_z$
$2D_x + 4D_y + 2D_z$	3	$(4/15)q_xq_z\gamma_x\gamma_z$	$-(2/15)q_xq_z\gamma_x\gamma_z$
$2D_x + 2D_y + 4D_z$	3	$(4/15)q_xq_y\gamma_x\gamma_y$	$-(2/15)q_xq_y\gamma_x\gamma_y$
$2D_x + 2D_y$	3	0.0	0.0
$2D_x + 2D_z$	3	0.0	0.0
$2D_y + 2D_z$	3	0.0	0.0
$4D_x + 4D_y + 4D_z$	1	0.0	0.0

Also listed are the preexponentials for the fluorescence intensity in both the parallel and perpendicular direction as calculated with the jump model.

SIMULATION RESULTS

We have also verified our results by a Monte Carlo simulation of the 90° jump model on a Compaq Deskpro 386-20 computer. We begin with a randomly distributed ensemble of 1,000,000 identical molecules, each with one fixed absorption dipole and one fixed emission dipole. The excitation probability of each dipole is $\cos^2\theta_0$, where θ_0 is the angle between the molecule's absorption dipole and the laboratory z-axis. Then each molecule is allowed to rotate about its principal axes with a probability $P_{i+} = \Delta t R_{i+}$, where R_{i+} is the rate of rotation about axis i in the plus direction. Thus there are six probabilities of rotation, one in each direction for each of the three principal rotation axes of the molecule. The approximation for this conversion from rates to probabilities is valid when Δt is small enough so that the total probability of all rotations is < 0.25. That is, fewer than one-quarter of all molecules undergo a rotation during any one time-step. We then loop through all of the molecules and calculate the intensity projection of each emission dipole in both the parallel and perpendicular directions of the lab frame. We must multiply each of these intensities by the excitation probability for that molecule. All of the parallel intensities are summed, as are the perpendicular ones, and these summations are the $I_{\parallel}$ and $I_{\perp}$ values used to calculate the anisotropy (Eq. 8) for each time step. We then loop through the time steps until the anisotropy goes to zero. These calculations agree precisely with our eigenvalue calculation of the jump model.

DISCUSSION

In this section we will address the differences between the two methods of describing fluorescence depolarization, and the physical mechanisms and assumptions behind each approach. In particular, we will consider under which conditions the difference between the two models can be best observed, and discuss the physical picture behind each model. The role and expected results of a master equation, in which a distribution of jump sizes governs the rotational motion, will be discussed. We will also examine the temperature dependence of the anisotropy decay rates and steady-state anisotropy of each approach, and comment on the application of the discon-

tinuous jump model to restricted motions, particularly the motion of a residue in a protein matrix.

Can the difference in decay rates between the two models be observed?

Although our solution is not strictly applicable to process that are diffusional or processes that proceed by a series of jumps between random orientations, the difference between the aligned and the nonaligned case found in the compartmental approach is significant. As a result of our derivation, one should be able to distinguish between nonsymmetric molecular systems undergoing either diffusion or large jumps between compartments simply by observing a single anisotropy decay in contrast with the method proposed by Valiev and Ivanov (19), which requires two different observations. For the general case with five exponential terms, the two methods do give slightly different solutions to the nonaligned problem; however, it is difficult to find a situation to distinguish between the two general solutions experimentally due to several factors. First, there are few molecules with so little symmetry that they would actually yield all five exponential terms in the anisotropy decay. One such system would be a large nonsymmetric molecule with an external probe attached in a nonaligned direction. For large molecules, we would expect the motion to be in small increments and thus follow the results of the diffusion equation. Molecules of the size where relatively large jumps would be expected to significantly contribute to the anisotropy decay invariably have too much symmetry to observe all five terms. Second, the values of some of the rotational rates are degenerate within the resolution of current instrumentation unless the molecule is highly anisotropic (i.e., the rotational rates all differ by about a factor of 10). For a molecule to be highly anisotropic, it must be large. The final reason is that the time scale to resolve five different exponentials must be within the fluorescent lifetime of the probe. Any motion that is considerably slower than the total intensity decay will not be resolved and will manifest itself as a higher limiting anisotropy. Techniques for expanding the observable range often introduce at least as many problems as they solve. However, in principle, it is possible to isolate one of the cross terms' rotational correlation time. Consider a molecule with cylindrical symmetry where $D_x = D_y \equiv D_\perp$, $D_z \equiv D_\parallel$, and the dipole is not aligned with any of the principal axes. Due to this symmetry, we can define our molecular axes so that $\gamma_y = 0$. This now leaves three terms in the anisotropy decay: $6\,D_\perp$, $2\,D_\perp + 4\,D_\parallel$, which are the same in both models, and one cross term with rotational correlation rate $5\,D_\perp + D_\parallel$ in the diffusion equation model, $6\,D_\perp + 2\,D_\parallel$ in the jump model. With the further assumption of $q_x = q_y$, we see that the prexponential of the second term is zero, thus leaving only two exponential terms:

$$r(t) = 0.1(3q_z^2 - 1)(3\,\gamma_z^2)e^{6D_\perp t} + 0.3(4\gamma_x\gamma_z q_x q_z)e^{D_c t}, \quad (11)$$

where D_c is $5\,D_\perp + D_\parallel$ for the diffusion equation model, and $6\,D_\perp + 2\,D_\parallel$ for the jump model. This cross term has the larger preexponential factor of the two exponentials, and should dominate the observed anisotropy decay. For example, if both absorption and emission dipoles have equal components in the x- and z-directions, the preexponentials are 0.05 for the common rate and 0.3 for the cross term. If we choose a molecule where $D_\parallel \gg D_\perp$, the rotational correlation rate of the cross term will differ by a factor of nearly two between the two models. Under the above molecular conditions, there is a large measurable difference in the anisotropy decay depending on which model is assumed. Although our compartmental derivation is not a random walk problem in the orientational space, we believe the difference outlined above should still be visible in the case of a distribution of steps of different sizes (19).

Different physical assumptions of the two approaches

The microscopic physical assumptions of each model are different. In the diffusion equation it is assumed that all motions are small and that each new orientation is close to the previous one. In our compartmental model we assume all rotations are exactly 90° and only along the principal axes, which is not a likely physical situation. However, the difference in the general solutions under the two assumptions may indicate that the diffusion equation approach is not always adequate to describe fluorescence polarization in certain physical systems. We propose that both approaches are only limiting cases of an underlying general principle governing molecular reorientation. That is, the true motion of a free molecular rotation is neither diffusive nor jump, but rather a distribution of different size motions represented by a master equation. The formalism and some simple examples of the rotational random walk problem with a distribution of jump sizes is presented by Valiev and Ivanov (19), although they do not apply their results to the case of fluorescence depolarization.

Another question is what is the physical relationship between the jump rates in the compartmental model and the rotational diffusion constants. We know that for 90° jumps they are mathematically identical in some "degenerate" cases (7, 13). The compartmental model treats depolarization as a process of exchange of dipole orientations. The macroscopic relaxation rate of a return to

equilibrium of a system that has been displaced from the thermodynamic equilibrium is related to the microscopic rate of exchange by the fluctuation–dissipation theorem. In a fluorescence depolarization experiment the displacement from equilibrium occurs only through an entropic term (i.e., we create order in the system by photoselection). The elementary physical process responsible for the anisotropy decay is the same process responsible for the exchange of orientations. The jump rate (the microscopic rate) should be identical to the rotational relaxation rate (the macroscopic rate). However, the macroscopic decay rates differ between the two approaches. This result implies that the observation of fluorescence depolarization is not directly related to the exchange of orientations in general, although it may coincide for some symmetric cases.

The different physical assumptions and consequences of the two models are considered below for some specific cases.

Restricted rotations

There are many systems of biological interest where only some particular orientations are possible due to molecular constraints (e.g., motions of residues in a protein and of probes in locally oriented systems such as membranes). For these situations, it appears that the discontinuous jump model should be the choice for describing fluorescence depolarization. In these cases, the elementary process of orientation exchange can be treated as the rate of transition over a barrier, and all the thermodynamics (temperature, pressure dependence) of this process, as far as is known, can be included in the calculation of the anisotropy decay. In addition, we can model small movements within a particular orientation by defining the entries of the **P** vectors to be distributions and not discrete values. In this case, we simply integrate the eigenvector component times the probabilities within a compartment in Eqs. 5 and 6.

Distribution of relatively large jumps

Although our derivation of fluorescence depolarization has been obtained for true molecular motion, fluorescence anisotropy decay can also occur due to other processes, such as energy transfer, with no involvement of molecular reorientation. Our approach is of course applicable to this case and it is easy to devise situations in which large jumps in the emission dipole orientation can occur in the energy transfer example.

Temperature behavior of the anisotropy decay in the two models

To examine the temperature characteristics of the two models, it is easiest to consider the steady-state anisotropy and use the Perrin plot, which is the inverse of the steady-state anisotropy versus temperature divided by viscosity (21). The temperature behavior of rotational diffusion rates has been established to be linear with temperature divided by viscosity (T/η). This is the Stokes–Einstein relationship, which comes from the assumption that the driving force of the rotational motions is the osmotic pressure of the solvent (22). To derive the relation between the rates in a jump model, we assume the jumps to occur over a barrier of height ΔH. With this assumption we must start with the Kramer's relation in the high viscosity limit:

$$D = \frac{D_0}{\eta} e^{-\Delta H/RT}, \tag{12}$$

where $D_0 = \nu\nu_0\rho$; with ν_0, the frequency at the bottom of the barrier (the curvature of the potential well); ν, the frequency factor at the top of the barrier; and ρ, the molecular density. This relation is clearly not linear in T, but over the range of T/η up to 1,000 K/cP, it is indeed a linear function of T/η. This property arises from the observation (23) that over a restricted temperature range the viscosity can be expanded as:

$$\eta = \eta_0 e^{E/RT}, \tag{13}$$

where η_0 and E are dependent upon the particular solvent. This relation is not exact but holds over the temperature range around room temperature (−30°C to 30°C). Typical values for glycerol–water mixtures are $\eta_0 = 10^{-9}$ cP and E/R = 8,000 K. Using this phenomenological expression for η, a plot of D versus T/η is linear for any reasonable value of ΔH (up to 50 RT). The range that can be explored experimentally is clearly within this limit. Consequently, the slope of the Perrin plot with rates described by Eqs. 12 and 13 is independent of ΔH and E. Instead, the slope of this line is approximately proportional only to D_0, which is made up solely of viscosity independent properties. This is in agreement with the results of the Perrin equation which uses the slope of this graph to determine the value of the "density" of the rotating particles. For unrestricted motions, the temperature dependence of the two models should be identical if the viscosity of the solvent is described by Eq. 13. For restricted motions (e.g., residues in proteins), it is not clear if Eq. 13 is still valid, and therefore, in that particular case, it may be possible to obtain information about the value of ΔH. Recent work by Weber has attempted to interpret data in this fashion to give insight into the local motions of residues within proteins (24).

The authors wish to thank Prof. Gregorio Weber for inspiring this work and for his many helpful discussions, and Prof. Michael Weissman for his discussions about this manuscript.

This work has been supported by grant PHS-1P41 RR03155 from the National Institutes of Health.

Received for publication 20 March 1989 and in final form 21 August 1989.

REFERENCES

1. Munro, I., I. Pecht, and L. Stryer. 1979. Subnanosecond motions of tryptophan residues in proteins. *Proc. Natl. Acad. Sci. USA.* 76:56–60.
2. Harris, D., L. McIntosh, and B. Hudson. 1986. Fluorescence lifetime and anisotropy studies of T4 lysozyme mutants containing single tryptophan residues. *Biophys. J.* 49:490*a*. (Abstr.)
3. Gratton, E., J. R. Alcala, and G. Marriott. 1986. Rotations of tryptophan residues in proteins. *Biochem. Soc. Trans.*14:835–838.
4. Ameloot, M., H. Hendrickx, W. Herreman, H. Pottel, F. Van Cauwelaert and W. van der Meer. 1984. Effect of orientational order on the decay of fluorescence anisotropy in membrane suspensions. *Biophys. J.*46:525–539.
5. Arcioni, A., F. Bertinelli, R. Tarroni, and C. Zannoni. 1987. Time resolved fluorescence depolarization in a nematic liquid crystal. *Mol. Physiol.* 61:1161–1181.
6. Tao, T. 1969. Time-dependent fluorescence depolarization and Brownian rotational diffusion coefficients of macromolecules. *Biopolymers.* 8:609–632.
7. Weber, G. 1971. Theory of fluorescence depolarization by anisotropic Brownian rotations. Discontinuous distribution approach. *J. Chem. Phys.* 55:2399–2411.
8. Favro, L. D. 1960. Theory of the rotational Brownian motion of a free rigid body. *Phys. Rev.* 119:53–62.
9. Belford, G. G., R. L. Belford, and G. Weber. 1972. Dynamics of fluorescence polarization in macromolecules. *Proc. Natl. Acad. Sci. USA.* 69:1392–1393.
10. Chaung, T.-J., and K. B. Eisenthal. 1972. Theory of fluorescence depolarization by anisotropic rotational diffusion. *J. Chem. Phys.* 57:5094–5097.
11. Ehrenberg, M., and R. Rigler. 1972. Polarized fluorescence and rotational brownian motion. *Chem. Phys. Lett.* 14:539–544.
12. Harvey, S. C., and H. Cheung. 1972. Computer simulation of fluorescence depolarization due to Brownian motion. *Proc. Natl. Acad. Sci. USA.* 69:3670–3672.
13. Piston, D. W., T. Bilash, and E. Gratton. 1989. Compartmental analysis of fluorescence anisotropy: perylene in viscous solvents. *J. Phys. Chem.* 93:3963–3967.
14. Razi-Naqvi, I. 1987. A new look at fluorescence depolarization and the dynamics of anisotropic rotational diffusion. *Chem. Phys. Lett.* 136:407–412.
15. Kauzmann, W. 1942. Dielectric relaxation as a chemical rate process. *Rev. Mod. Phys.* 14:12–44.
16. Van Vleck, J. H., and V. F. Weisskopf. 1945. On the shape of collision-broadened lines. *Rev. Mod. Phys.* 17:227–236.
17. Cross, A. C., D. H. Waldek, and G. Flemming. 1983. Time resolved polarization spectroscopy: level kinetics and rotational diffusion. *J. Chem. Phys.* 78:6455–6467.
18. Szabo, A. 1984. Theory of fluorescence depolarization in macromolecules and membranes. *J. Chem. Phys.* 81:150–187.
19. Valiev, K. A., and E. N. Ivanov. 1973. Rotational Brownian motion. *Sov. Phys. Usp.* 16:1–16.
20. Jacquez, J. A. 1985. Compartmental Analysis in Biology and Medicine. University of Michigan Press, Ann Arbor. 560 pp.
21. Perrin, F. 1942. Polarization of light scattered by isotropic opalescent media. *J. Chem. Phys.* 10:415–427.
22. Einstein, A. 1905. On the movement of small particles suspended in a stationary liquid demanded by the molecular-kinetic theory of heat. *Ann. Phys.* 17:549-556.
23. Miner, C. S., and N. N. Dalton, eds. 1953. *Glycerol.* Reinhold Publishing Corp., New York. 282–284.
24. Weber, G. 1989. Perrin revisited: parametric theory of the motional depolarization of fluorescence. *J. Phys. Chem.* 93:6069–6073.